Journal of Tissue Engineering
3(1) 2041731412466405

DOI: 10.1177/2041731412466405
tej.sagepub.com
SAGE

In vitro chondrogenic differentiation of human adipose-derived stem cells with silk scaffolds

Hyeon Joo Kim[1], Sang-Hyug Park[2,4], Jennah Durham[1], Jeffrey M Gimble[3], David L Kaplan[2] and Jason L Dragoo[1]

Abstract

Human adipose-derived stem cells have shown chondrogenic differentiation potential in cartilage tissue engineering in combination with natural and synthetic biomaterials. In the present study, we hypothesized that porous aqueous-derived silk protein scaffolds would be suitable for chondrogenic differentiation of human adipose-derived stem cells. Human adipose-derived stem cells were cultured up to 6 weeks, and cell proliferation and chondrogenic differentiation were investigated and compared with those in conventional micromass culture. Cell proliferation, glycosaminoglycan, and collagen levels in aqueous-derived silk scaffolds were significantly higher than in micromass culture. Transcript levels of SOX9 and type II collagen were also upregulated in the cell–silk constructs at 6 weeks. Histological examination revealed that the pores of the silk scaffolds were filled with cells uniformly distributed. In addition, chondrocyte-specific lacunae formation was evident and distributed in the both groups. The results suggest the biodegradable and biocompatible three-dimensional aqueous-derived silk scaffolds provided an improved environment for chondrogenic differentiation compared to micromass culture.

Keywords

cartilage, adipose-derived stem cells, silk scaffolds, chondrogenic differentiation

Introduction

Due to its avascularity and low biosynthetic activity, articular cartilage has limited self-regenerative capacity after tissue damage as a result of trauma, developmental anomalies, or progressive degeneration such as osteoarthritis.[1,2] Several therapies have been attempted to repair cartilage defects, including curettage, transplantation of chondrocytes, and drilling through the subchondral bone.[3–6] Although these therapies provide some benefits, the outcomes are generally less satisfactory because the repair tissue often resembles fibrocartilage rather than hyaline cartilage. In recent years, cell-based articular cartilage tissue engineering has proved to be a promising alternative therapy for repairing damaged cartilage by combining chondrogenic cells, biomaterial scaffolds, and suitable culture conditions.[7,8]

Chondrocytes and stem cells are commonly used for cartilage tissue engineering. Previously, autologous chondrocytes were preferred, but present studies have suggested that autologous cells have additional problems of dedifferentiation upon increased passaging for cell expansion, donor site limitation, and morbidity.[7,9] Recently, many studies have indicated that human adipose-derived stem cells (hASCs) can easily be obtained from liposuction waste or arthroscopy, and maintained in a stable undifferentiated state during in vitro expansion. These cells have the capacity to differentiate into cartilage, bone, muscle, and adipose lineages.[7,9–13] Although some studies suggest that hASCs may have limited chondrogenic potential and might not be suitable for cartilage regeneration,[14,15] several studies have shown the in vivo and in vitro chondrogenic differentiation potential of hASCs in cartilage tissue engineering approaches using natural and synthetic scaffolds.[16–19]

[1]Department of Orthopaedic Surgery, Stanford University School of Medicine, Palo Alto, CA, USA
[2]Department of Biomedical Engineering, Tufts University, Medford, MA, USA
[3]Pennington Biomedical Research Center, Louisiana State University System, Baton Rouge, LA, USA
[4]Department of Biomedical Engineering, Jungwon University, 85, Munmu-ro, Goesan-eup, Goesan-gun, Chungbuk, Republic of Korea

Corresponding author:
Jason L Dragoo, Department of Orthopaedic Surgery, Stanford University School of Medicine, Palo Alto, CA 94305, USA.
Email: jdragoo@stanford.edu

Silk, a unique family of proteins derived from silkworms and spiders, is a novel protein-based polymeric biomaterial with impressive mechanical properties, biocompatibility, and biodegradability.[20–22] Previous studies have reported in vitro cartilage tissue engineering of bone marrow–derived stem cells (BMSCs) and embryonic stem cell-derived mesenchymal stem cells using three-dimensional (3D) degradable silk-based scaffolds.[23–25]

In the present study, we hypothesized that hASCs could be suitable for chondrogenic differentiation using porous aqueous-derived silk scaffolds. The chondrogenic differentiation potential of hASCs in aqueous-derived silk scaffolds was compared with conventional micromass culture techniques.

Materials and methods

Materials

Fetal bovine serum (FBS), low-glucose Dulbecco's modified Eagle medium (DMEM), antibiotic–antimycotic, trypsin–ethylenediaminetetraacetic acid (EDTA), Trizol reagent, and Quant-iT PicoGreen dsDNA Assay kit were obtained from Invitrogen Corporation (Carlsbad, CA, USA). Ascorbic acid and insulin–transferrin–selenium (ITS)+1 (1.0 mg/mL insulin from bovine pancreas, 0.55 mg/mL human transferring, 0.5 µg/mL sodium selenite, 50 mg/mL bovine serum albumin, and 470 µg/mL linoleic acid) were obtained from Sigma (St. Louis, MO, USA). All other substances were of analytical or pharmaceutical grade and were obtained from Sigma. Transforming growth factor-β1 (TGF-β1) was obtained from R&D systems (Minneapolis, MN, USA). Silkworm cocoons were kindly supplied by Tajimia Shoji Co. (Yokohama, Japan).

Preparation of scaffolds

Aqueous-derived silk fibroin scaffolds were prepared by adding 4 g of granular NaCl (particle size; 710–850 µm) into 2 mL of 6 wt% silk fibroin solution in disk-shaped Teflon containers (1.8 cm in diameter × 2 cm in height) based on previously published procedures.[21,26] The containers were covered and left at room temperature for 24 h, and then immersed in water and the NaCl extracted for 2 days. The porosity of the aqueous-derived silk scaffolds was ~96%, and the compressive strength and modulus were 58 ± 3 and 670 ± 30 kPa, respectively.[26]

hASCs expansion

Isolated hASCs, as described by McIntosh et al.,[27] were cultured in low-glucose DMEM supplemented with 10% FBS and 1% antibiotic–antimycotic. Media were replenished every 3 days, and cells were passaged at 80% confluence using trypsin–EDTA. The initial passage of the primary cell culture was referred to as passage 0 (P0).

Cell seeding on the silk scaffolds and in vitro culture

For examination of cell growth and differentiation in vitro on the silk scaffolds, passage 2 (P2) hASCs (1×10^6 cells/scaffold) were seeded onto prewetted (DMEM, overnight) scaffolds (5 mm diameter × 3 mm thick). The constructs were placed into 24-well plates. Cells were allowed to attach for 2 h. The constructs were placed in a humidified incubator at 37°/5% CO_2. Medium was replaced at a rate of 50% every 2–3 days for 6 weeks. Chondrogenic medium consisted of low-glucose DMEM supplemented with 1% FBS, 1% antibiotic–antimycotic, 50 µg/mL ascorbic acid, 1% ITS+1, and 10 ng/mL TGF-β1.

Micromass culture

P2 hASCs were placed in a 15 mL polypropylene tube at a density of 1×10^6 cells/mL and harvested by centrifugation for 5 min at 500g. Cell pellets in the tubes were cultured in chondrogenic medium (see section "Cell seeding on the silk scaffolds and in vitro culture") for 6 weeks. Tube caps were loosened in order to maintain 37°C and 5% CO_2. Medium was replaced at a rate of 50% every 2–3 days.

Biochemical analysis

For DNA content, four constructs per group and time points were minced with microscissors on ice. DNA content was measured using the PicoGreen assay (Invitrogen Corporation), according to the manufacturer's protocol. Samples were measured fluorometrically at an excitation wavelength of 480 nm and an emission wavelength of 528 nm. The amount of glycosaminoglycan (GAG) was measured using the 1,9-dimethylmethylene blue (DMB; Sigma) assay.[28,29] Samples (N = 4) were digested for 16 h with papain digestion solution (125 µg/mL papain, 5 mM L-cystein, 100 mM Na_2HPO_4, 5 mM EDTA, pH 6.2) at 60°C. Individual samples were mixed with the DMB solution, and absorbance was measured at 525 nm. Total GAG content of each sample was extrapolated using standard plots of shark chondroitin sulfate (Sigma). Collagen content was measured using a modified Hride Tullberg–Reinert method.[30] Digested samples were dried at 37°C in 96-well plates for 24 h and reacted with a dye solution for 1 h with mild shaking. The dye solution (pH 3.5) was prepared with Sirius red dissolved in picric acid–saturated solution (1.3%) at 1 mg/mL. After washing five times with 0.01 N HCl, the dye–sample complex was resolved in 0.1 N NaOH. Absorbance was read at 550 nm. Total collagen content of each sample was extrapolated using a standard plot of bovine collagen (Sigma).

RNA isolation, real-time reverse transcription polymerase chain reaction

Total RNA from constructs (N = 4 per group) was extracted using Trizol reagent (Invitrogen Corporation), and the

isolated RNA concentration and quality were determined using a spectrophotometer. Quantitative real-time reverse transcription polymerase chain reaction (RT-PCR) assays for aggrecan, type I collagen, type II collagen, SOX9, and glyceraldehyde-3-phosphate dehydrogenase (GAPDH) transcripts were carried out using gene-specific double-fluorescence-labeled probes in a 7900 Sequence Detector (PE Applied Biosystems, Foster City, CA, USA). Probes and primers for these genes were obtained from PE Applied Biosystems as Assays-On-Demand gene expression products. Briefly, the RNA samples were reverse transcribed into cDNA using High Capacity cDNA Reverse Transcription Kit, according to the manufacturer's protocol (Applied Biosystems). Real-time PCR amplification was performed in a 384-well plate with a 13 µL of reaction mixture. The thermal cycling conditions were 2 min at 50°C and 10 min at 95°C, followed by 50 cycles of 15 s of denaturation at 95°C and 1 min of annealing and extension at 60°C. The comparative threshold[6] PCR cycle detection method (ΔΔCt method) that compares the differences in Ct values of hASCs and treated groups was used to calculate the relative fold change in gene expression. All experiments were carried out in quadruple for each condition.

Histological evaluation

After fixation with 10% neutral-buffered formalin for at least 24 h, specimens (N = 4 per group and time point) were embedded within paraffin and sectioned at 5 µm thickness. For histological evaluation, sections were deparaffinized, rehydrated trough a series of graded ethanol, and stained with Alcian blue (pH 2.5) with hematoxylin counterstaining.

Statistical analysis

Repeated measures analysis of variance (ANOVA), using post hoc Dunnett's multiple comparison method, was used to determine the p-value. Results were considered significant at $p < 0.05$. All values are expressed as mean ± standard deviation.

Results

Biochemical analysis

The DNA content of the cell–silk constructs was significantly higher than those of micromass culture at 3 and 6 weeks after cell seeding ($p < 0.05$) (Figure 1). In the micromass culture, similar cell proliferation was observed at 3 and 6 weeks ($p < 0.05$), while cell proliferation in the cell–silk constructs decreased at 6 weeks compared to 3 weeks ($p < 0.05$). The GAG level in cell–silk constructs produced at 3 and 6 weeks was 41% ($p < 0.05$) and 53% greater ($p < 0.05$), respectively, than in the micromass cultures (Figure 2). However, GAG synthesis in micromass cultures at 3 versus 6 weeks and in cell–silk constructs at 3 versus 6 weeks was not significantly. Total collagen level in the cell–silk constructs was sixfold to sevenfold higher ($p < 0.05$) than in micromass; however, there was no significant difference within the micromass and cell–silk construct groups at 3 versus 6 weeks (Figure 3).

Expression of chondrogenic differentiation-associated genes

After 3 weeks of culture, transcript levels of SOX9, type II collagen, and type I collagen were statistically similar in

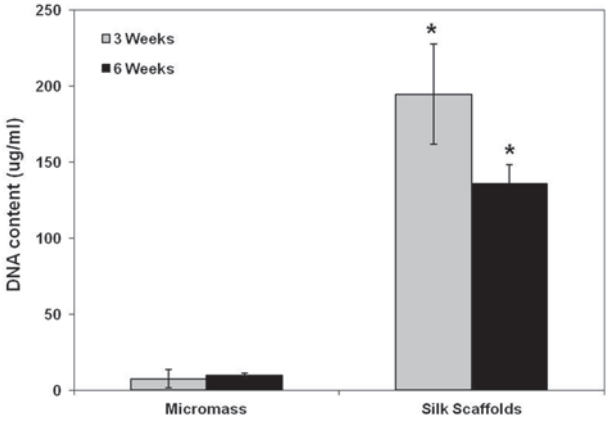

Figure 1. Proliferation of hASCs. Proliferation of hASCs in the aqueous-derived 3D scaffolds and micromass cultures determined by DNA assay using the PicoGreen assay. Data are shown as mean ± standard deviation from four samples. The symbol "*" represents statistically significant differences ($p < 0.05$).
hASC: human adipose-derived stem cell; 3D: three-dimensional.

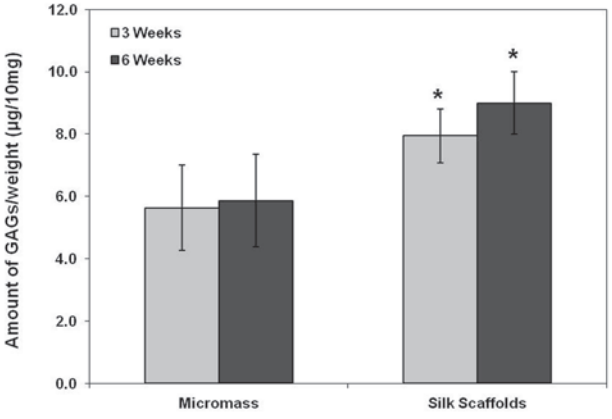

Figure 2. Synthesis of glycosaminoglycans (GAGs). The amount of GAG in samples measured by the 1,9-dimethylmethylene blue (DMB) assay. Data are shown as mean ± standard deviation from four samples. The symbol "*" represents statistically significant differences ($p < 0.05$).

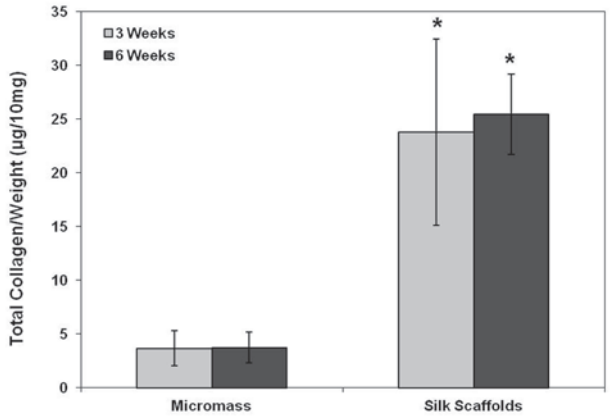

Figure 3. Measurement of total collagen. The amount of total collagen measured by the Hride Tullberg–Reinert method. Data are shown as mean ± standard deviation from four samples. The symbol "*" represents statistically significant differences ($p < 0.05$).

both groups of cultures. However, the levels of SOX9, type II collagen, and type I collagen transcripts were significantly upregulated ($p < 0.05$) in the cell–silk constructs at 6 weeks (Figure 4) in comparison to micromass culture. Expression of aggrecan in the cell–silk constructs was higher ($p < 0.05$) than in micromass culture at 3 weeks, and the expression increased in both groups at 6 weeks, with 32% greater ($p < 0.05$) expression in the cell–silk constructs than in micromass culture (Figure 4(a)).

Histological observations

The accumulation of a major component of the extracellular matrix (ECM) proteoglycan was examined by alcian blue staining at 6 weeks (Figure 5). Histological examination revealed that pores were filled with cells, and the cells were uniformly distributed in the cell–silk constructs at 6 weeks (Figure 5(c) and (d)). Moreover, chondrocyte-specific lacunae formation was evident and distributed in the both

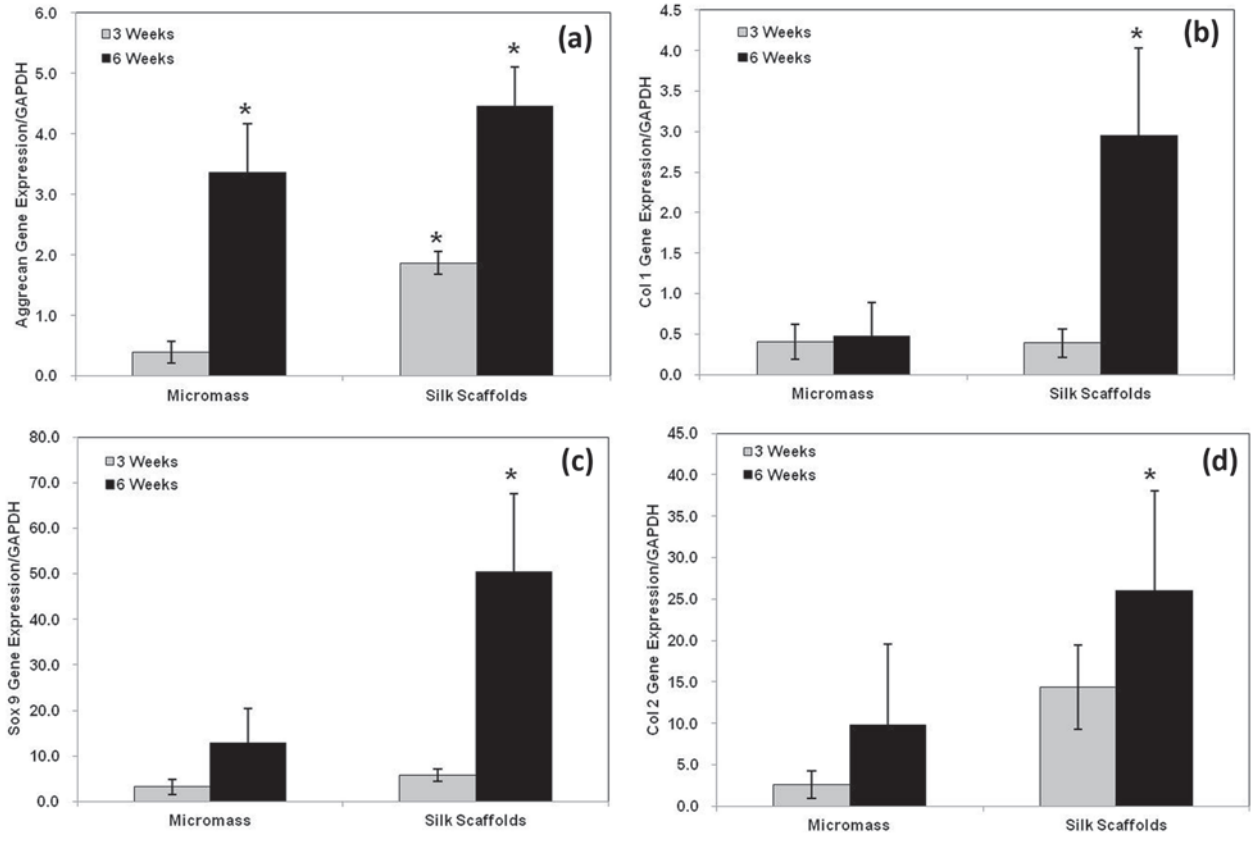

Figure 4. Expression of RNA transcripts related to chondrogenic differentiation. Transcript expression of several chondrogenic differentiation markers quantified by real-time RT-PCR. a; Aggrecan Gene Expression, b; Type I Collagen Gene Expression, c; Sox 9 Gene Expression, d; Type II Collagen Gene Expression. Transcript levels were normalized by GAPDH. Data are shown as mean ± standard deviation from four samples. The symbol "*" represents statistically significant differences ($p < 0.05$).
RT-PCR: reverse transcription polymerase chain reaction; GAPDH: glyceraldehyde-3-phosphate dehydrogenase.

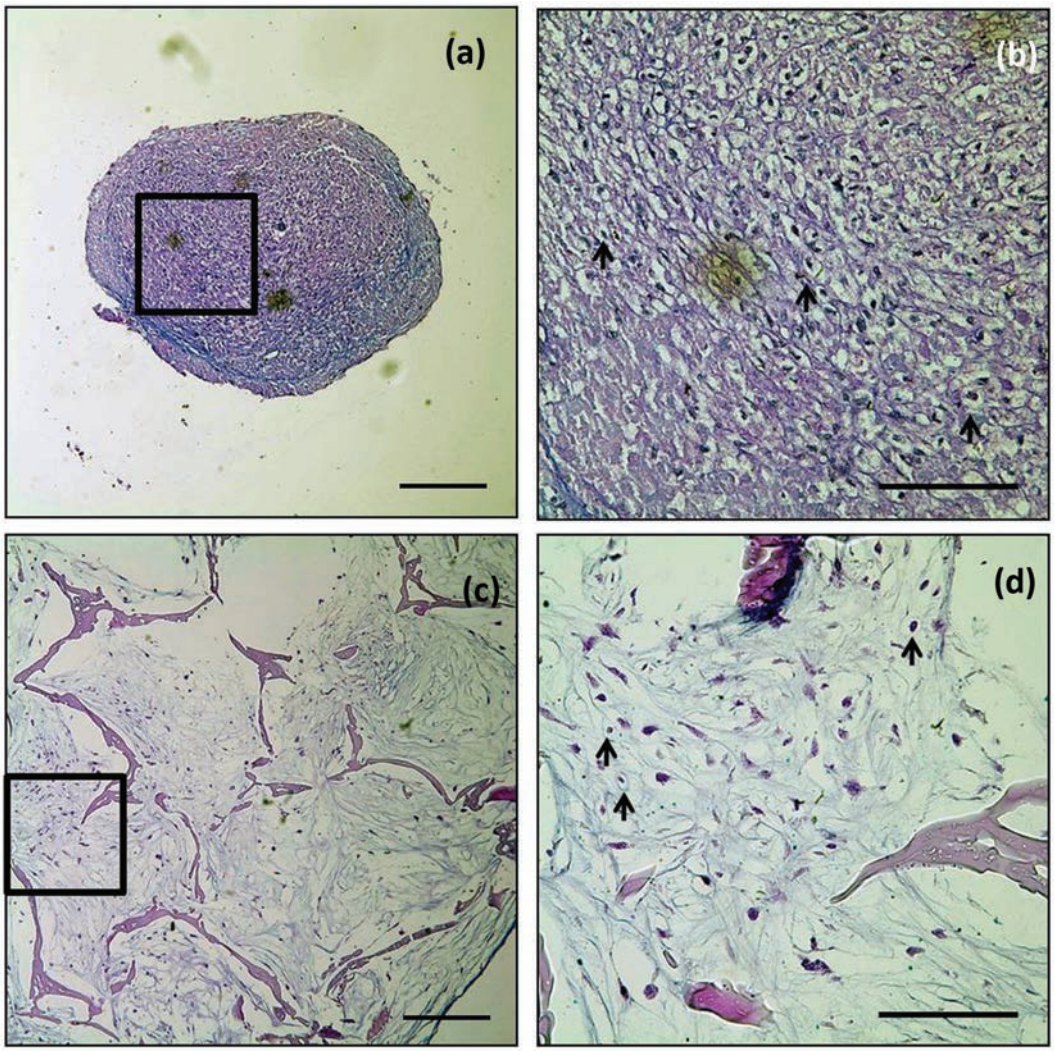

Figure 5. Alcian blue staining. (a and b) Micromass cultures and (c and d) constructs of silk with hASCs cultured for 6 weeks. Extracellular matrices of proteoglycan (blue) were detected in the both groups. Arrow (→) indicates examples of chondrocyte-specific lacunae. Scale bars indicate 250 μm (a and c; 10×) and 100 μm (b and d; 40×).

groups of cultures. Alcian blue staining was more intense in micromass than in the cell–silk constructs; however, this staining difference did not correlate with GAG quantitation data (see earlier section).

Discussion

The field of tissue engineering involving hASCs is rapidly advancing and offers the possibility of regeneration of tissues damaged by disease or trauma.[18,31] hASCs have high proliferative and multilineage potential, including chondrogenesis, and can be obtained in abundance from fat tissue with minimal injury.[13,17,32,33] Guilak et al. showed that hASCs possess the ability to synthesize cartilage matrix proteins if cultured in a 3D matrix in the presence of specific soluble mediators (TGF-β and dexamethasone).[34]

Although previous studies suggested that BMSCs are more suitable than hASCs for chondrogenesis,[35] several studies have shown the chondrogenic differentiation potential of hASCs in cartilage tissue engineering.[16–19] Previous studies also showed that hASCs retain strong proliferation ability, maintain their phenotypes, and have strong multidifferentiation potential.[36–38] In this study, we observed that gene expression for aggrecan and type II collagen were upregulated in both micromass and silk 3D scaffolds. However, transcript levels were higher in silk 3D matrices than in micromass culture. SOX9, a key transcription factor in chondrogenesis,[8] was also upregulated in cell–silk constructs at 6 weeks.

It is well known that type I collagen is associated with the dedifferentiation process during monolayer expansion of chondrocytes, and its presence is a poor indicator of

articular ECM-like matrix.[39] However, Barry et al.[40] showed that type I collagen was uniformly detected in undifferentiated cells and throughout differentiation. Therefore, significance of the detection of type I collagen expression in the silk 3D matrices needs to be further elucidated.

Silkworm silk fibroin has been used commercially as biomedical sutures for decades and in textile production for centuries. Silkworm silk from *Bombyx mori* consists of heavy and light chain polypeptides of ~350 and ~25 kDa, respectively, connected by a disulfide link.[26,41,42] These core fibers are encased in a sericin coat, a family of glue-like proteins. The sericin glue-like proteins are the major cause of adverse problems with biocompatibility and hypersensitivity to silk.[20,43] Sericins are the water soluble and extractable by boiling. After sericins were removed, throughout the period of implantation, silk scaffolds were well tolerated by the host animals, and immune responses to the implants were mild.[44] Fibroin is a protein dominated in composition by the amino acids glycin, alanine, and serine that form antiparallel β-sheets in the spun fibers, leading to the stability and mechanical features of the fibers.[45,46] The unique strength and resistance to mechanical compression,[20,47] biocompatibility,[48–51] the slow rate of degradation,[52–54] the utility of this protein in various forms for tissue engineering soft,[55,56] and hard[21,26,57] tissue suggest this biomaterial as a suitable substrate for tissue engineering.

A number of methods, such as salt leaching, gas forming, or freeze-drying, have been reported to generate porous 3D matrices from natural and synthetic polymers.[26] In this study, porous aqueous-derived silk scaffolds were prepared using a salt leaching method, and the pore size and the porosity of the scaffolds were regulated by the granular NaCl size for supporting hASC differentiation. One previous study has illustrated that normal appearing articular cartilage is similar to porous aqueous-derived silk scaffolds with respect to mechanical properties.[58] Compressive moduli were 581 ± 17 and 670 ± 30 kPa for human knee articular cartilage[58] and 6 wt% silk fibroin porous aqueous-derived scaffolds,[26] respectively. Therefore, the mechanical properties of porous biodegradable polymeric scaffolds are favorable for cartilage tissue engineering. Other studies supported good cell adhesion and growth on aqueous-derived silk 3D scaffolds because of its rougher surface structure.[21] The high porosity (>90%) and interconnected porous network are also desirable for ingrowth of cells and synthesis of ECM.[59] The porosity percentage (96%), pore size (650 ± 50), and modulus (670 ± 30 KPa) of the aqueous-derived silk scaffolds appeared to support hASC chondrogenic differentiation to a greater degree than micromass culture at 6 weeks.

The present study shows that hASCs in biodegradable and biocompatible 3D aqueous-derived silk scaffolds may be useful for tissue engineered cartilage regeneration. Cell growth, GAG production, and chondrogenic differentiation-associated gene expression in the silk scaffolds groups were statistically greater compared with micromass culture. The scaffolds appeared to provide a suitable environment for hASC survival and chondrogenesis. Further investigation into the mechanical properties and in vivo behavior of these hASC–silk scaffold constructs will be necessary to fully evaluate its potential for use in tissue engineering.

Funding

This research received no specific grant from any funding agency in the public, commercial, or not-for-profit sectors.

References

1. Hunziker EB. Articular cartilage repair: basic science and clinical progress. A review of the current status and prospects. *Osteoarthritis Cartilage* 2002; 10(6): 432–463.
2. Moutos FT and Guilak F. Functional properties of cell-seeded three-dimensionally woven poly(epsilon-caprolactone) scaffolds for cartilage tissue engineering. *Tissue Eng Part A* 2010; 16(4): 1291–1301.
3. Ficat RP, Ficat C, Gedeon P, et al. Spongialization: new treatment for diseased patellae. *Clin Orthop Relat Res* 1979; 144: 74–83.
4. Mitchell N and Shepard N. Resurfacing of adult rabbit articular cartilage by multiple perforations through subchondral bone. *J Bone Joint Surg Am* 1976; 58(2): 230–233.
5. Levy AS, Lohnes J, Sculley S, et al. Chondral delamination of the knee in soccer players. *Am J Sports Med* 1996; 24(5): 634–639.
6. Breinan HA, Minas T, Hsu HP, et al. Effect of cultured autologous chondrocytes on repair of chondral defects in a canine model. *J Bone Joint Surg Am* 1997; 79(10): 1439–1451.
7. Wei YY, Hu HY, Wang HQ, et al. Cartilage regeneration of adipose-derived stem cells in a hybrid scaffold from fibrin-modified PLGA. *Cell Transplant* 2009; 18(2): 159–170.
8. Sa-Lima H, Caridade SG, Mano JF, et al. Stimuli-responsive chitosan-starch injectable hydrogels combined with encapsulated adipose-derived stromal cells for articular cartilage regeneration. *Soft Matter* 2010; 6(20): 5184–5195.
9. Han YS, Wei YY, Wang SS, et al. Enhanced chondrogenesis of adipose-derived stem cells by the controlled release of transforming growth factor-beta 1 from hybrid microspheres. *Gerontology* 2009; 55(5): 592–599.
10. Mahmoudifar N and Doran PM. Chondrogenic differentiation of human adipose-derived stem cells in polyglycolic acid mesh scaffolds under dynamic culture conditions. *Biomaterials* 2010; 31(14): 3858–3867.
11. Estes BT, Diekman BO, Gimble JM, et al. Isolation of adipose-derived stem cells and their induction to a chondrogenic phenotype. *Nat Protoc* 2010; 5(7): 1294–1311.
12. Cheng NC, Estes BT, Awad HA, et al. Chondrogenic differentiation of adipose-derived adult stem cells by a porous scaffold derived from native articular cartilage extracellular matrix. *Tissue Eng Part A* 2009; 15(2): 231–241.
13. Dragoo JL, Lieberman JR, Lee RS, et al. Tissue-engineered bone from BMP-2-transduced stem cells derived from human fat. *Plast Reconstr Surg* 2005; 115(6): 1665–1673.

14. Huang JI, Kazmi N, Durbhakula MM, et al. Chondrogenic potential of progenitor cells derived from human bone marrow and adipose tissue: a patient-matched comparison. *J Orthop Res* 2005; 23(6): 1383–1389.
15. Afizah H, Yang Z, Hui JHP, et al. A comparison between the chondrogenic potential of human bone marrow stem cells (BMSCs) and adipose-derived stem cells (ADSCs) taken from the same donors. *Tissue Eng* 2007; 13(4): 659–666.
16. Dragoo JL, Carlson G, McCormick F, et al. Healing full-thickness cartilage defects using adipose-derived stem cells. *Tissue Eng* 2007; 13(7): 1615–1621.
17. Jiang T, Liu W, In XJ, et al. Potent in vitro chondrogenesis of CD105 enriched human adipose-derived stem cells. *Biomaterials* 2010; 31(13): 3564–3571.
18. Rada T, Reis RL and Gomes ME. Adipose tissue-derived stem cells and their application in bone and cartilage tissue engineering. *Tissue Eng Part B Rev* 2009; 15(2): 113–125.
19. Awad HA, Wickham MQ, Leddy HA, et al. Chondrogenic differentiation of adipose-derived adult stem cells in agarose, alginate, and gelatin scaffolds. *Biomaterials* 2004; 25(16): 3211–3222.
20. Altman GH, Diaz F, Jakuba C, et al. Silk-based biomaterials. *Biomaterials* 2003; 24(3): 401–416.
21. Kim HJ, Kim UJ, Vunjak-Novakovic G, et al. Influence of macroporous protein scaffolds on bone tissue engineering from bone marrow stem cells. *Biomaterials* 2005; 26(21): 4442–4452.
22. Kim HJ, Kim HS, Matsumoto A, et al. Processing windows for forming silk fibroin biomaterials into a 3D porous matrix. *Aust J Chem* 2005; 58(10): 716–720.
23. Meinel L, Hofmann S, Karageorgiou V, et al. Engineering cartilage-like tissue using human mesenchymal stem cells and silk protein scaffolds. *Biotechnol Bioeng* 2004; 88(3): 379–391.
24. Wang YZ, Kim UJ, Blasioli DJ, et al. In vitro cartilage tissue engineering with 3D porous aqueous-derived silk scaffolds and mesenchymal stem cells. *Biomaterials* 2005; 26(34): 7082–7094.
25. Tigli RS, Cannizaro C, Gumusderelioglu M, et al. Chondrogenesis in perfusion bioreactors using porous silk scaffolds and hESC-derived MSCs. *J Biomed Mater Res A* 2011; 96(1): 21–28.
26. Kim UJ, Park J, Kim HJ, et al. Three-dimensional aqueous-derived biomaterial scaffolds from silk fibroin. *Biomaterials* 2005; 26(15): 2775–2785.
27. McIntosh K, Zvonic S, Garrett S, et al. The immunogenicity of human adipose-derived cells: temporal changes in vitro. *Stem Cells* 2006; 24(5): 1246–1253.
28. Whitley CB, Ridnour MD, Draper KA, et al. Diagnostic-test for mucopolysaccharidosis. 1. Direct method for quantifying excessive urinary glycosaminoglycan excretion. *Clin Chem* 1989; 35(3): 374–379.
29. Muller G and Hanschke M. Quantitative and qualitative analyses of proteoglycans in cartilage extracts by precipitation with 1,9-dimethylmethylene blue. *Connect Tissue Res* 1996; 33(4): 243–248.
30. Tullberg-Reinert H and Jundt G. In situ measurement of collagen synthesis by human bone cells with a sirius red-based colorimetric microassay: effects of transforming growth factor beta 2 and ascorbic acid 2-phosphate. *Histochem Cell Biol* 1999; 112(4): 271–276.
31. Langer R and Vacanti JP. Tissue engineering. *Science* 1993; 260(5110): 920–926.
32. Hedrick MH, Zuk PA, Zhu M, et al. Multilineage cells from human adipose tissue: implications for cell-based therapies. *Tissue Eng* 2001; 7(2): 211–228.
33. Aust L, Devlin B, Foster SJ, et al. Yield of human adipose-derived adult stem cells from liposuction aspirates. *Cytotherapy* 2004; 6(1): 7–14.
34. Guilak F, Erickson GR, Gimble JM, et al. Chondrogenic potential of adipose tissue-derived stromal cells in vitro and in vivo. *Biochem Biophys Res Commun* 2002; 290(2): 763–769.
35. Hui JHP, Afizah H, Yang Z, et al. A comparison between the chondrogenic potential of human bone marrow stem cells (BMSCs) and adipose-derived stem cells (ADSCs) taken from the same donors. *Tissue Eng* 2007; 13(4): 659–666.
36. Zhu Y, Liu T, Song K, et al. Adipose-derived stem cell: a better stem cell than BMSC. *Cell Biochem Funct* 2008; 26(6): 664–675.
37. Cowan CM, Shi YY, Aalami OO, et al. Adipose-derived adult stromal cells heal critical-size mouse calvarial defects. *Nat Biotechnol* 2004; 22(5): 560–567.
38. Guilak F, Lott KE, Awad HA, et al. Clonal analysis of the differentiation potential of human adipose-derived adult stem cells. *J Cell Physiol* 2006; 206(1): 229–237.
39. Trzeciak T and Richter M. [Biomaterials in articular cartilage lesions repair]. *Chir Narzadow Ruchu Ortop Pol* 2008; 73(2): 107–111.
40. Barry F, Boynton RE, Liu BS, et al. Chondrogenic differentiation of mesenchymal stem cells from bone marrow: differentiation-dependent gene expression of matrix components. *Exp Cell Res* 2001; 268(2): 189–200.
41. Tanaka K, Kajiyama N, Ishikura K, et al. Determination of the site of disulfide linkage between heavy and light chains of silk fibroin produced by *Bombyx mori*. *Biochim Biophys Acta* 1999; 1432(1): 92–103.
42. Zhou CZ, Confalonieri F, Medina N, et al. Fine organization of *Bombyx mori* fibroin heavy chain gene. *Nucleic Acids Res* 2000; 28(12): 2413–2419.
43. Wen CM, Ye ST, Zhou LX, et al. Silk-induced asthma in children: a report of 64 cases. *Ann Allergy* 1990; 65(5): 375–378.
44. Wang Y, Rudym DD, Walsh A, et al. In vivo degradation of three-dimensional silk fibroin scaffolds. *Biomaterials* 2008; 29(24–25): 3415–3428.
45. He SJ, Valluzzi R and Gido SP. Silk I structure in *Bombyx mori* silk foams. *Int J Biol Macromol* 1999; 24(2–3): 187–195.
46. Asakura T, Yao JM, Yamane T, et al. Heterogeneous structure of silk fibers from *Bombyx mori* resolved by C-13 solid-state NMR spectroscopy. *J Am Chem Soc* 2002; 124(30): 8794–8795.
47. Sofia S, McCarthy MB, Gronowicz G, et al. Functionalized silk-based biomaterials for bone formation. *J Biomed Mater Res* 2001; 54(1): 139–148.
48. Setzen G and Williams EF. Tissue response to suture materials implanted subcutaneously in a rabbit model. *Plast Reconstr Surg* 1997; 100(7): 1788–1795.
49. Lee KY, Kong SJ, Park WH, et al. Effect of surface properties on the antithrombogenicity of silk fibroin/S-carboxymethyl

kerateine blend films. *J Biomater Sci Polym Ed* 1998; 9(9): 905–914.
50. Santin M, Motta A, Freddi G, et al. In vitro evaluation of the inflammatory potential of the silk fibroin. *J Biomed Mater Res* 1999; 46(3): 382–389.
51. Panilaitis B, Altman GH, Chen JS, et al. Macrophage responses to silk. *Biomaterials* 2003; 24(18): 3079–3085.
52. Lam KH, Nijenhuis AJ, Bartels H, et al. Reinforced poly(L-lactic acid) fibers as suture material. *J Appl Biomater* 1995; 6(3): 191–197.
53. Rossitch E, Bullard DE and Oakes WJ. Delayed foreign-body reaction to silk sutures in pediatric neurosurgical patients. *Childs Nerv Syst* 1987; 3(6): 375–378.
54. Soong HK and Kenyon KR. Adverse reactions to virgin silk sutures in cataract-surgery. *Ophthalmology* 1984; 91(5): 479–483.
55. Altman GH, Horan RL, Lu HH, et al. Silk matrix for tissue engineered anterior cruciate ligaments. *Biomaterials* 2002; 23(20): 4131–4141.
56. Chen JS, Altman GH, Karageorgiou V, et al. Human bone marrow stromal cell and ligament fibroblast responses on RGD-modified silk fibers. *J Biomed Mater Res A* 2003; 67(2): 559–570.
57. Meinel L, Karageorgiou V, Hofmann S, et al. Engineering bone-like tissue in vitro using human bone marrow stem cells and silk scaffolds. *J Biomed Mater Res A* 2004; 71(1): 25–34.
58. Jurvelin JS, Buschmann MD and Hunziker EB. Mechanical anisotropy of the human knee articular cartilage in compression. *Proc Inst Mech Eng H* 2003; 217(3): 215–219.
59. Katoh K, Tanabe T and Yamauchi K. Novel approach to fabricate keratin sponge scaffolds with controlled pore size and porosity. *Biomaterials* 2004; 25(18): 4255–4262.